

# Simple regularization scheme for multi-reference density functional theories

W. Satuła<sup>1,2</sup> and J. Dobaczewski<sup>1,2,3</sup>

<sup>1</sup>*Institute of Theoretical Physics, Faculty of Physics,  
University of Warsaw, ul. Hoża 69, PL-00-681 Warsaw, Poland*

<sup>2</sup>*Helsinki Institute of Physics, P.O. Box 64, FI-00014 University of Helsinki, Finland*

<sup>3</sup>*Department of Physics, P.O. Box 35 (YFL), University of Jyväskylä, FI-40014 Jyväskylä, Finland*

(Dated: July 4, 2014)

**Background:** Extensions of single-reference (SR) energy-density-functionals (EDFs) to multi-reference (MR) applications involve using the generalized Wick theorem (GWT), which leads to singular energy kernels that cannot be properly integrated to restore symmetries, unless the EDFs are generated by *true* interactions.

**Purpose:** We propose a new method to regularize the MR EDFs, which is based on using auxiliary quantities obtained by multiplying the kernels with appropriate powers of overlaps.

**Methods:** Regularized matrix elements of two-body interactions are obtained by integrating the auxiliary quantities and then solving simple linear equations.

**Results:** We implement the new regularization method within the self-consistent Skyrme-Hartree-Fock approach and we perform a proof-of-principle angular-momentum projection (AMP) of states in odd-odd nucleus <sup>26</sup>Al. We show that for EDFs generated by *true* interactions, our regularization method gives results identical to those obtained within the standard AMP procedure. We also show that for EDFs that do not correspond to *true* interactions, it gives stable and converging results that are different than unstable and non-converging standard AMP values.

**Conclusions:** The new regularization method proposed in this work may provide us with a relatively inexpensive and efficient tool to generalize SR EDFs to MR applications, thus allowing for symmetry restoration and configuration mixing performed for typical nuclear EDFs, which most often do not correspond to *true* interactions.

PACS numbers: 21.60.Jz, 21.30.Fe,

## I. INTRODUCTION

Density Functional Theory (DFT) is a universal approach used in quantum chemistry, molecular physics, and condensed matter physics to calculate properties of electronic systems. Its extension to nuclear physics is by no means trivial, encountering difficulties associated in part with the binary composition of atomic nuclei, spin-dependent interactions, superfluidity, and strong surface effects. Major difference between the electronic and nuclear DFT is associated with the lack of external binding potential, as atomic nuclei are self-bound systems, and with the saturation of nuclear interactions at a given value of density. This implies that the nuclear DFT must necessarily be formulated in terms of intrinsic, and not laboratory densities, which, in turn, leads to the spontaneous breaking of fundamental symmetries.

In spite of these difficulties, the nuclear DFT is the microscopic tool of choice to study in a systematic manner medium-mass and heavy nuclei. In the symmetry-broken mean-field variant, often referred to as single-reference (SR) DFT, the method has proven to be extremely successful in reproducing and predicting bulk nuclear properties like masses, quadrupole moments, or nuclear radii. However, for a precise description of numerous observables, the SR nuclear DFT is inadequate. In particular, at the SR level, matrix elements of electromagnetic transitions or beta decays can only be treated within a quasiclassical approximation. Fully quantal calculations of such observables are impossible without the symme-

try restoration, which requires extensions from the SR to multi-reference (MR) DFT.

However, within the MR DFT, implementation of the symmetry restoration is plagued with technical and conceptual difficulties [1–3]. The reason is that the SR DFT, serving as the starting point, is usually derived from an effective, density-dependent pseudo-potential, and is therefore not directly related to a Hamiltonian. The only reasonable, and to a large extent unambiguous generalization of the SR energy density functional (EDF) to the MR level is possible within the generalized Wick’s theorem (GWT) [4] that establishes a one-to-one correspondence between the SR and MR functionals. In such an implementation, the MR EDF retains the form of the underlying SR EDF, but is solely expressed in terms of the so-called transition densities. Unfortunately, the resulting MR EDFs are, in general, singular and require regularization. In spite of preliminary attempts, concentrating mostly on a direct removal of self-pairing effects [2, 3], the problem of regularization still lacks satisfactory and practical solution. The aim of this work is to propose such a solution.

The paper is organized as follows. In Sec. II A, we recall the standard formulation of the MR DFT scheme based on the GWT, and we identify sources of potential pathologies. Then, in subsections II B and II C we present two variants of the new regularization scheme, hereafter called linear (LR) and quadratic regularization (QR), respectively. Our method is illustrated by applications to the angular-momentum projection (AMP) prob-

lem, but can similarly be used to restore other broken symmetries. In particular, the particle-number restoration within the pairing-plus-quadrupole Hamiltonian is currently studied in Ref. [5]. Summary and perspectives are discussed in Sect. III.

## II. REGULARIZATION SCHEME

### A. Standard MR DFT scheme

In this work, all implementations of projection methods are based on the GWT, which allows for deriving compact and numerically tractable expressions for off-diagonal matrix elements between Slater determinants. For an arbitrary Slater determinant  $|\Psi\rangle$ , by  $|\tilde{\Psi}\rangle = \hat{R}(\Omega)|\Psi\rangle$  we denote the one that is rotated in space, gauge space, or isospace, for the angular-momentum, particle-number, or isospin restoration, respectively. Hereafter, we focus our attention on the AMP, but the presented ideas and methodology can be rather straightforwardly generalized to the particle-number [5] or isospin projections.

In order to bring forward the origin of singularities in energy kernels [1–3], it is instructive to recall principal properties of the standard GWT approach. Let us start with a one-body density-independent operator  $\hat{F} = \sum_{ij} F_{ij} a_i^\dagger a_j$ . Its off-diagonal kernel (the matrix element divided by the overlap), can be calculated with the aid of GWT, and reads [4]:

$$\frac{\langle \Psi | \hat{F} | \tilde{\Psi} \rangle}{\langle \Psi | \tilde{\Psi} \rangle} = \sum_{ij} F_{ij} \overline{a_i^+ a_j} \equiv \sum_{ij} F_{ij} \tilde{\rho}_{ji}, \quad (1)$$

where

$$\tilde{\rho}_{ji} \equiv \overline{a_i^+ a_j} \equiv \frac{\langle \Psi | a_i^+ a_j | \tilde{\Psi} \rangle}{\langle \Psi | \tilde{\Psi} \rangle}, \quad (2)$$

denotes transition density matrix. Therefore, its matrix element between the unprojected state  $|\Psi\rangle$  and AMP state  $|IMK\rangle = \hat{P}_{MK}^I |\Psi\rangle$  can be calculated from

$$\begin{aligned} F_{IMK} &\equiv \langle \Psi | \hat{F} \hat{P}_{MK}^I | \Psi \rangle = \\ &= \frac{2I+1}{8\pi^2} \int d\Omega D_{MK}^{I*}(\Omega) \langle \Psi | \hat{F} | \tilde{\Psi} \rangle, \end{aligned} \quad (3)$$

where

$$\hat{P}_{MK}^I = \frac{2I+1}{8\pi^2} \int D_{MK}^{I*}(\Omega) \hat{R}(\Omega) d\Omega \quad (4)$$

is the AMP operator,  $D_{MK}^I(\Omega)$  is the Wigner function, and  $\hat{R}(\Omega) = e^{-i\alpha\hat{I}_z} e^{-i\beta\hat{I}_y} e^{-i\gamma\hat{I}_z}$  stands for the active rotation operator in space, parametrized in terms of Euler angles  $\Omega = (\alpha, \beta, \gamma)$ , and  $M$  and  $K$  denote the angular-momentum components along the laboratory and intrinsic  $z$ -axis, respectively [6, 7].

The immediate conclusion stemming from Eqs. (1)–(2) is that the overlaps, which appear in the denominators of the matrix element and transition density matrix, cancel out, and the matrix element  $\langle \Psi | \hat{F} | \tilde{\Psi} \rangle$  of an arbitrary one-body density-independent operator  $\hat{F}$  is free from singularities and can be safely integrated, as in Eq. (3).

Let us now turn our attention to two-body operators. The most popular two-body effective interactions used in nuclear structure calculations are the zero-range Skyrme [8, 9] and finite-range Gogny [10] effective forces. Because of their explicit density dependence, they should be regarded, for consistency reasons, as generators of two-body part of the nuclear EDF. The transition matrix element of the two-body generator reads:

$$\langle \Psi | \hat{V}_{2B} | \tilde{\Psi} \rangle = \frac{1}{4} \sum_{ijkl} \bar{V}_{ijkl}[\tilde{\rho}] \langle \Psi | a_i^+ a_j^+ a_l a_k | \tilde{\Psi} \rangle, \quad (5)$$

where  $\bar{V}_{ijkl}[\tilde{\rho}]$  denotes the antisymmetrized transition-density-dependent matrix element. Gogny and Skyrme effective interactions both contain local terms proportional to  $\rho^\eta$  which, in the MR DFT formulation, are usually replaced with the transition (mixed) density  $\rho^\eta \rightarrow \tilde{\rho}^\eta$  [11]. Such a procedure, although somewhat arbitrary, is very common, because it fulfills a set of internal consistency criteria formulated in Refs. [12, 13]. These include hermiticity, independence of scalar observables on the orientation of the intrinsic system, and consistency with the underlying mean field. The alternative way of proceeding is to substitute density-dependent terms with projected density [14] or average density [15]. These scenarios do not fulfill the consistency criteria and will not be discussed here.

Evaluating the transition matrix element, Eq. (5), with the aid of GWT, one obtains,

$$\begin{aligned} \frac{\langle \Psi | \hat{V}_{2B} | \tilde{\Psi} \rangle}{\langle \Psi | \tilde{\Psi} \rangle} &= \frac{1}{4} \sum_{ijkl} \bar{V}_{ijkl}[\tilde{\rho}] \left( \overline{a_i^+ a_j^+} \overline{a_l a_k} \right. \\ &\quad \left. + \overline{a_i^+ a_k} \overline{a_j^+ a_l} - \overline{a_i^+ a_l} \overline{a_j^+ a_k} \right). \end{aligned} \quad (6)$$

Furthermore, for particle-number-conserving theory, contractions  $\overline{a_i^+ a_j^+}$  and  $\overline{a_l a_k}$  vanish, whereas the remaining two contractions give products of two transition density matrices,

$$\frac{\langle \Psi | \hat{V}_{2B} | \tilde{\Psi} \rangle}{\langle \Psi | \tilde{\Psi} \rangle} = \frac{1}{4} \sum_{ijkl} \bar{V}_{ijkl}[\tilde{\rho}] (\tilde{\rho}_{ki} \tilde{\rho}_{lj} - \tilde{\rho}_{li} \tilde{\rho}_{kj}), \quad (7)$$

or

$$\begin{aligned} \frac{\langle \Psi | \hat{V}_{2B} | \tilde{\Psi} \rangle}{\langle \Psi | \tilde{\Psi} \rangle} &= \frac{1}{4} \sum_{ijkl} \bar{V}_{ijkl}[\tilde{\rho}] \left( \frac{\langle \Psi | a_i^+ a_k | \tilde{\Psi} \rangle \langle \Psi | a_j^+ a_l | \tilde{\Psi} \rangle}{\langle \Psi | \tilde{\Psi} \rangle^2} \right. \\ &\quad \left. - \frac{\langle \Psi | a_i^+ a_l | \tilde{\Psi} \rangle \langle \Psi | a_j^+ a_k | \tilde{\Psi} \rangle}{\langle \Psi | \tilde{\Psi} \rangle^2} \right), \end{aligned} \quad (8)$$

that is, the transition matrix element reads

$$\langle \Psi | \hat{V}_{2B} | \tilde{\Psi} \rangle = \frac{1}{2} \sum_{ijkl} \bar{V}_{ijkl} [\bar{\rho}] \frac{\langle \Psi | a_i^\dagger a_k | \tilde{\Psi} \rangle \langle \Psi | a_j^\dagger a_l | \tilde{\Psi} \rangle}{\langle \Psi | \tilde{\Psi} \rangle} \quad (9)$$

This defines the matrix element between the unprojected and AMP states,

$$V_{IMK}^{2B} \equiv \langle \Psi | \hat{V}_{2B} \hat{P}_{MK}^I | \Psi \rangle = \frac{2I+1}{8\pi^2} \int d\Omega D_{MK}^{I*}(\Omega) \langle \Psi | \hat{V}_{2B} | \tilde{\Psi} \rangle. \quad (10)$$

At variance with the one-body case discussed above, the integrand in Eq. (10) is inversely proportional to the overlap, thus containing potentially dangerous (singular) terms. The singularity disappears only if the sums in the numerator, evaluated at angles  $\Omega$  where the overlap  $\langle \Psi | \tilde{\Psi} \rangle$  equals zero, give a vanishing result; such a cancellation requires evaluating the numerator without any approximations or omitted terms. An additional singularity is created by the density dependence of the interaction.

If some approximation of the numerator is involved, the leading-order singularity goes as:

$$\langle \Psi | \hat{V}_{2B} | \tilde{\Psi} \rangle \sim \frac{1}{\langle \Psi | \tilde{\Psi} \rangle^{1+\eta}}, \quad (11)$$

with the term  $1/6 \leq \eta \leq 1$  inherited from the direct density dependence of the Gogny or Skyrme effective forces which are, as already mentioned, commonly used to generate the modern non-relativistic nuclear EDFs. This singularity precludes, in general, determination of the integral in Eq. (10). Only in special cases, e.g., for signature-symmetry conserving states in even-even nuclei [16, 17], the overlaps never vanish and the problem does not appear.

Thus, the GWT formulation of MR DFT is, in general, singular. In fact, it is well defined only for  $\hat{V}_{2B}$  being a *true* interaction. An example of such an EDF generator is the density-independent Skyrme interaction  $SV_T$ , which is the SV interaction of Ref. [18] with all the EDF tensor terms included (these were omitted in the original definition of SV). Interaction  $SV_T$  was recently used to calculate the isospin-symmetry-breaking corrections to superallowed  $0^+ \rightarrow 0^+$   $\beta$ -decay by means of the isospin- and angular-momentum projected DFT formalism [19].

Progress in development of projection techniques and difficulties in working out reliable regularization schemes for density-dependent interactions [2] increased the demand for density-independent effective interactions and stimulated vivid activity in this field resulting in developing density-independent zero-range [20, 21] as well as finite-range [22] forces. The spectroscopic quality of these new forces is, however, still far from satisfactory. In addition, the technology of performing beyond-mean-field calculations with these novel interactions is being developed only now [23, 24].

The pathologies arising in the GWT description of the two-body energy kernels come from uncompensated zeros of the overlap matrix. The central idea of this work

is to cure the problem by replacing the calculation of projected matrix elements with higher-order quantities, which are regularized by multiplying the integrands with an appropriately chosen power of the overlap:

$$\langle \Psi | \hat{V}_{2B} | \tilde{\Psi} \rangle \rightarrow \langle \Psi | \hat{V}_{2B} | \tilde{\Psi} \rangle \langle \Psi | \tilde{\Psi} \rangle^n. \quad (12)$$

The proposed regularization scheme amounts to replacing the calculation of matrix elements  $V_{IMK}^{2B}$ , given in Eq. (10), by the calculation of an auxiliary quantities defined as:

$$V_{IMK}^{2B,n} = \frac{2I+1}{8\pi^2} \int d\Omega D_{MK}^{I*}(\Omega) \langle \Psi | \hat{V}_{2B} | \tilde{\Psi} \rangle \langle \Psi | \tilde{\Psi} \rangle^n. \quad (13)$$

The central assumption behind such a regularization method is that the two-body matrix element  $\langle \Psi | \hat{V}_{2B} | \tilde{\Psi} \rangle$  is regularizable, meaning that there exists a regularization procedure allowing for removal of singularities and replacing the infected matrix elements by regular ones,

$$\langle \Psi | \hat{V}_{2B} | \tilde{\Psi} \rangle \longrightarrow \widetilde{\langle \Psi | \hat{V}_{2B} | \tilde{\Psi} \rangle}, \quad (14)$$

for which the projected matrix elements can be calculated as in Eq. (10),

$$\tilde{V}_{IMK}^{2B} = \frac{2I+1}{8\pi^2} \int d\Omega D_{MK}^{I*}(\Omega) \widetilde{\langle \Psi | \hat{V}_{2B} | \tilde{\Psi} \rangle}, \quad (15)$$

and which, in turn, can be expanded on a series of the Wigner  $D$ -functions:

$$\widetilde{\langle \Psi | \hat{V}_{2B} | \tilde{\Psi} \rangle} = \sum_{I'M'K'} \tilde{V}_{I'M'K'}^{2B} D_{M'K'}^{I'}(\Omega). \quad (16)$$

Indeed, by inserting expansion (16) into Eq. (15), and employing the orthonormality conditions of the Wigner  $D$ -functions [7], one straightforwardly obtains the desired result.

Finally, the regularized matrix elements  $\widetilde{\langle \Psi | \hat{V}_{2B} | \tilde{\Psi} \rangle}$  are determined by requesting that the auxiliary quantities (13), calculated before and after regularization are equal, that is,

$$V_{IMK}^{2B,n} \equiv \tilde{V}_{IMK}^{2B,n}. \quad (17)$$

for

$$\tilde{V}_{IMK}^{2B,n} = \frac{2I+1}{8\pi^2} \int d\Omega D_{MK}^{I*}(\Omega) \widetilde{\langle \Psi | \hat{V}_{2B} | \tilde{\Psi} \rangle} \langle \Psi | \tilde{\Psi} \rangle^n. \quad (18)$$

Let us underline that our method does not require any explicit *a priori* knowledge of the regularization scheme. Also note that the expansion coefficients  $\tilde{V}_{IMK}^{2B}$ , appearing in Eqs. (15) and (16), represent *true* regularized (two-body) matrix elements.

Two variants of such a regularization scheme, dubbed linear regularization (LR) and quadratic regularization (QR), corresponding to, respectively,  $n = 1$  and  $n = 2$ , are discussed below in Secs. II B and II C.

## B. Linear regularization scheme

The LR scheme applies, for example, to the density-independent SV interaction in its original formulation [18], that is, without the EDF tensor terms. It is also applicable to the density-dependent SIII functional [18]. The reason is that the density-dependence of this latter force does not lead, for a given type of particles, to a higher power of density. The third example, where the LR should be sufficient, is the Coulomb exchange treated in the so called Slater approximation [25], because in this approximation the exchange Coulomb transition matrix element behaves as

$$\tilde{\rho}^{4/3} \langle \Psi | \tilde{\Psi} \rangle \sim \langle \Psi | \tilde{\Psi} \rangle^{-1/3}. \quad (19)$$

In cases when the LR scheme is sufficient to cancel all poles of the integrand, the set of auxiliary quantities  $V_{IMK}^{2B,1}$  (13) can be calculated, in principle exactly, using suitably chosen quadratures with sufficient number of integration nodes.

The overlap is always regular and, therefore, it can be expanded in terms of the Wigner  $D$ -functions as,

$$\langle \Psi | \tilde{\Psi} \rangle = \sum_{I''M''K''} c_{I''M''K''}^{\mathcal{N}} D_{M''K''}^{I''}(\Omega), \quad (20)$$

where

$$c_{IMK}^{\mathcal{N}} \equiv \langle \Psi | \hat{P}_{MK}^I | \Psi \rangle = \frac{2I+1}{8\pi^2} \int d\Omega D_{MK}^{I*}(\Omega) \langle \Psi | \tilde{\Psi} \rangle. \quad (21)$$

Substitution of expansions (16) and (20) into Eq. (18), taken at  $n = 1$ , leads to:

$$\tilde{V}_{IMK}^{2B,1} = \frac{2I+1}{8\pi^2} \sum_{I'M'K'} \tilde{V}_{I'M'K'}^{2B} \sum_{I''M''K''} c_{I''M''K''}^{\mathcal{N}} \int d\Omega D_{MK}^{I*}(\Omega) D_{M'K'}^{I'}(\Omega) D_{M''K''}^{I''}(\Omega). \quad (22)$$

In the case of  $I+I'+I''$  being half-integer, the integration over the single volume must be replaced by integration over the double volume [7]. The integral in Eq. (22) is equal [7] to

$$\begin{aligned} \frac{2I+1}{8\pi^2} \int d\Omega D_{MK}^{I*}(\Omega) D_{M'K'}^{I'}(\Omega) D_{M''K''}^{I''}(\Omega) \\ = \mathbf{C}_{I''M''I'M'}^{IM} \mathbf{C}_{I''K''I'K'}^{IK}, \end{aligned} \quad (23)$$

where symbols  $\mathbf{C}$  stand for the Clebsch-Gordan coefficients. The integral has the same form both for integer and half-integer angular momenta.

Inserting (23) to (22), and requesting that Eq. (17) holds at  $n = 1$ , gives rise to a set of linear equations for regularized matrix elements  $\tilde{V}_{I'M'K'}^{2B}$ :

$$V_{IMK}^{2B,1} = \sum_{I'M'K'} A_{I'M'K'}^{IMK} \tilde{V}_{I'M'K'}^{2B}, \quad (24)$$

where

$$A_{I'M'K'}^{IMK} = \sum_{I''M''K''} c_{I''M''K''}^{\mathcal{N}} \mathbf{C}_{I''M''I'M'}^{IM} \mathbf{C}_{I''K''I'K'}^{IK}. \quad (25)$$

Matrix  $A_{I'M'K'}^{IMK}$  is quadratic for even-even and odd-odd nuclei and rectangular for odd- $A$  nuclei. The problem of finding the regularized matrix elements within the LR scheme is thus reduced to calculating auxiliary quantities (13) for  $n = 1$  and then solving a set of linear equations (24). In the HFODD solver, the latter is handled by using the singular-value-decomposition (SVD) technique.

We note here that the regularization procedure can be applied separately to all terms of the EDF, that is, terms that correspond to interactions can be treated within the standard AMP method, and only those which do not, should be treated within the regularization scheme.

The expansion of Slater determinant  $|\Psi\rangle$  in terms of the AMP states reads [6],

$$|\Psi\rangle = \sum_{IK} |IKK\rangle = \sum_{IK} \hat{P}_{KK}^I |\Psi\rangle. \quad (26)$$

In turn, the sum rule, which connects mean-field averages and projected matrix elements, has the form

$$\langle \Psi | \hat{V}_{2B} | \Psi \rangle = \sum_{IK} \langle \Psi | \hat{V}_{2B} \hat{P}_{KK}^I | \Psi \rangle = \sum_{IK} V_{IKK}^{2B}. \quad (27)$$

The sum rule expresses the HF mean-field average value in terms of the projected matrix elements, and thus constitutes a stringent test of the performed AMP. On the one hand, when  $\hat{V}_{2B}$  is a *true* interaction, the sum rule must be strictly obeyed. On the other hand, for singular energy kernels, its violation gives a numerical estimate of problems related to not using *true* interactions. Similarly, the sum rule calculated for regularized matrix elements,

$$\langle \Psi | \hat{V}_{2B} | \Psi \rangle = \sum_{IK} \tilde{V}_{IKK}^{2B}, \quad (28)$$

tests the quality of the regularization procedure. Note that sum rules must be obeyed separately for all terms in the interaction, which allows for studying singularities of energy kernels of separate terms. In what follows, we show results obtained for the sum-rule residuals, that is, for differences between right- and left-hand sides of Eqs. (27) and (28). Apart from those, we also assess precision of the AMP by considering energy  $E_{I=0}$  of the lowest  $I = 0$  state.

More precisely, we focus our attention on investigating stability of these two quantities in function of the highest angular momentum  $I_{\max}$  included in the calculations, and we present them versus  $I_{\max}$ . The same value of  $I_{\max}$  is consistently used to define both summation ranges in Eqs. (24) and (25). Note that in Eq. (25), the range of summation should be higher than the natural cutoff dictated by the highest meaningful AMP components in the mean-field wave function, which are given by the values of amplitudes  $c_{IMK}^{\mathcal{N}}$ . With increasing values of  $I_{\max}$ , the

residuals of sum rules (27) and (28), should converge to zero.

All calculations were performed using the unrestricted-symmetry solver HFODD [26, 27]. We employed the Gauss-Chebyshev quadratures to integrate over the  $\alpha$  and  $\gamma$  Euler angles and the Gauss-Legendre quadrature to integrate over the  $\beta$  Euler angle. To achieve a sufficient accuracy, for each Euler angle we used a large number of mesh points equal  $N_\alpha = N_\beta = N_\gamma \equiv N = 50$ .

The examples presented below pertain to odd-odd nucleus  $^{26}\text{Al}$ , and to the so called anti-aligned mean-field configuration, which is relevant in the context of the superallowed Fermi  $\beta$ -decay [19]. The most demanding task was to calculate the auxiliary integrals  $V_{IMK}^{2B,1}$ , Eq. (13). Since we were interested in comparing the standard and regularized calculations, we decided to use a relatively small configuration space, consisting of only  $N_{\text{shell}} = 6$  spherical harmonic-oscillator shells. Such small space suppresses high angular-momentum components in the reference Slater determinant. Unless explicitly stated, in all calculations, in both direct and exchange channels the Coulomb interaction was treated exactly.

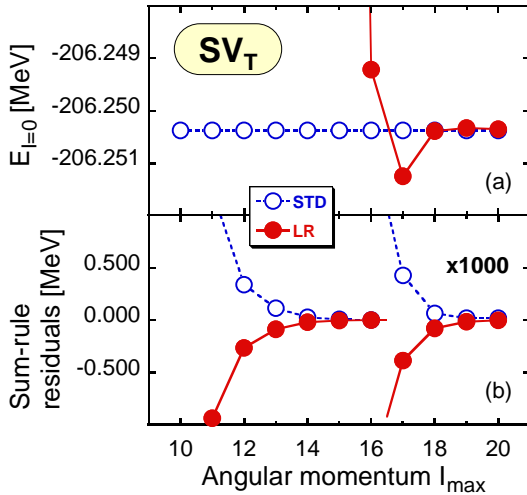


FIG. 1. (Color online) Convergence of the lowest  $I=0$  energy (top) and Skyrme-energy sum-rule residuals (bottom) in function of the highest angular momentum  $l_{\text{max}}$  included in the calculations. Open and full circles represent results obtained using the standard AMP method and our LR method, respectively. Calculations were performed for the *true* Skyrme interaction  $\text{SV}_T$  (that is, with the tensor EDF terms included).

It is instructive to begin the discussion by showing results for  $E_{I=0}$  and Skyrme-energy sum-rule residuals obtained for the  $\text{SV}_T$  Skyrme force. Such a calculation tests the numerical implementation of the method, and can be regarded as a proof of principle of the LR scheme. The reason is, as already mentioned, that the  $\text{SV}_T$  is a *true* interaction and, therefore, both standard AMP method and LR method should give exactly the same values of both indicators. As can be seen in Fig. 1, this is indeed the case. It turns out that for  $l_{\text{max}} \geq 10$ , the standard AMP values of  $E_{I=0}$  are perfectly stable (up to a fraction

of eV). However, the sum rule, which also tests the convergence of higher angular momenta, reaches a similar level of precision only above  $l_{\text{max}} = 20$ . The LR values of  $E_{I=0}$  converge only above  $l_{\text{max}} = 20$ , which illustrates the fact that in Eq. (24), higher intermediate angular momenta must be taken into account. Note, however, that the sum rules calculated using both methods converge in a similar smooth way.

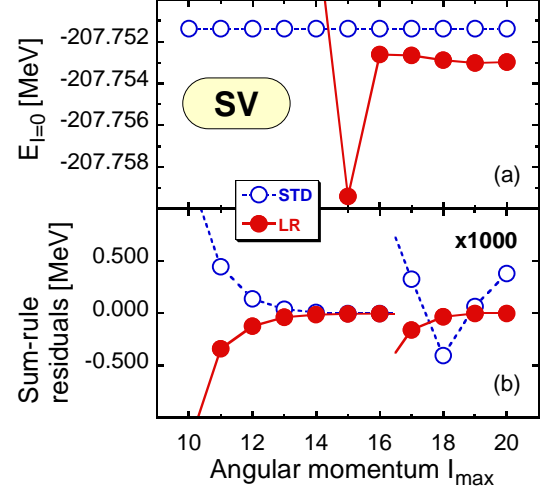


FIG. 2. (Color online) Same as in Fig. 1 but for the original Skyrme functional SV, that is, with the tensor EDF terms neglected.

The density-independent Skyrme parametrization SV in its original formulation [18], that is, without the tensor EDF terms, no longer corresponds to an interaction. Fig. 2 clearly shows that even such a seemingly insignificant departure from the *true* Hamiltonian is immediately detectable through the indicators tested in our study. In the standard AMP, energy  $E_{I=0}$  is again perfectly stable over the entire range of studied values of  $l_{\text{max}}$ . However, such stability can be misleading, because the LR value, which converges only at  $l_{\text{max}} = 20$ , differs by as much as 2 keV.

Note that the singularity of energy kernels leaves its fingerprint in the values of the standard-AMP sum-rule residuals. After an apparent convergence (at the level of a few keV), which is visible below  $l_{\text{max}} = 16$ , at the level of a few eV, this indicator, in fact, does not converge to zero. On the other hand, the LR sum-rule residuals smoothly converge to zero with high precision. An important conclusion obtained here is that the stability of the ground-state energy does not necessarily warrant that its value be free from spurious effects.

For the density-dependent SIII functional [18], problems encountered within the standard AMP are further magnified. In this example, we performed calculations using the Slater approximation [25] of the Coulomb exchange energy. Therefore, here we applied our LR method both to the Skyrme and Coulomb parts of the functional. The results are depicted in Fig. 3, showing

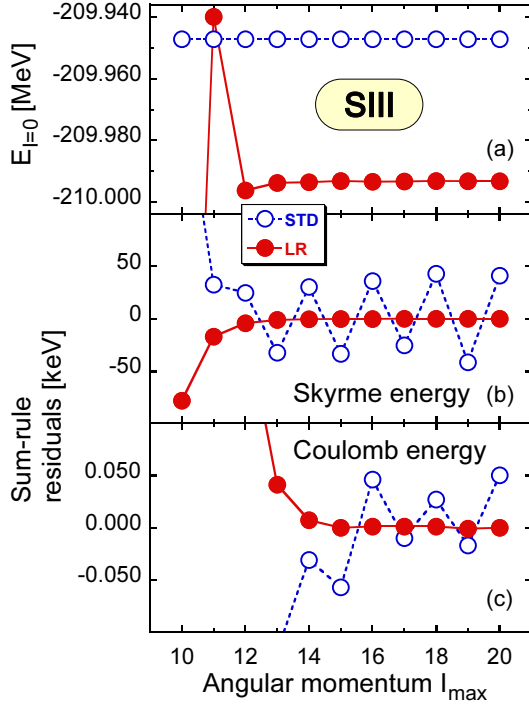


FIG. 3. Same as in Fig. 1 but for the original SIII Skyrme functional. Panels (b) and (c) show sum-rule residuals of the Skyrme and Coulomb energies, respectively. Slater approximation of the Coulomb exchange energy was used.

the energy  $E_{I=0}$  (upper panel), Skyrme-energy sum-rule residuals (middle panel), and Coulomb-energy sum-rule residuals (lower panel). Similarly as in Fig. 2, the standard AMP leads to misleadingly stable values of  $E_{I=0}$ ; however, now the corresponding sum rules turn out to be completely unstable. For the Skyrme and Coulomb energies, they stagger around zero at the level of 50 keV and 50 eV, respectively. In contrast, the LR method perfectly stabilizes the sum rules, which smoothly converge to zero, and leads to stable values of  $E_{I=0}$ . However, the LR  $E_{I=0}$  energy is now shifted down by almost 50 keV, as compared to the standard AMP solution.

Finally, let us point out yet another shortcoming of the standard AMP approach. Fig. 4 shows results of the test of stability of  $E_{I=0}$  with respect to the number of mesh points  $N$  used in numerical integrations over the Euler angles. In this example, calculations were performed for the SIII functional [18] and exact Coulomb exchange energy. It is clearly visible that the standard-AMP values of  $E_{I=0}$  vary strongly and quite erratically with  $N$ . This is owing to the fact that the results do depend on relative positions of mesh points with respect to singularities of the energy kernel. In contrast, the LR results are perfectly stable.

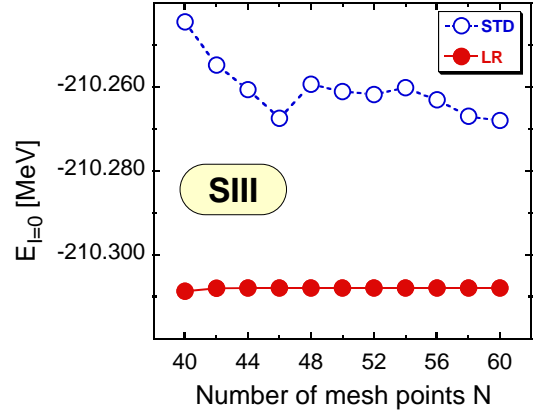


FIG. 4. (Color online) Energies  $E_{I=0}$  calculated using the standard AMP (open circles) and LR (full circles) methods, as functions of the number of mesh points  $N$ . Calculations were performed for the original SIII Skyrme functional. The maximum angular momentum of  $I_{\max} = 20$  was used.

### C. Quadratic regularization scheme

In the QR scheme, matrix element  $V_{IMK}^{2B}$  (10) is replaced by the auxiliary quantity  $V_{IMK}^{2B,2}$  defined in Eq. (13) for  $n = 2$ . Again we assume that matrix element  $\langle \Psi | \hat{V}_{2B} | \tilde{\Psi} \rangle$  is regularizable. Inserting expansions (16) and (20) into (13) gives

$$V_{IMK}^{2B,2} = \sum_{I_1 M_1 K_1} \tilde{V}_{I_1 M_1 K_1}^{2B} \sum_{I_2 M_2 K_2} c_{I_2 M_2 K_2}^{\mathcal{N}} \sum_{I_3 M_3 K_3} c_{I_3 M_3 K_3}^{\mathcal{N}} \frac{2I+1}{8\pi^2} \int d\Omega D_{MK}^{I*}(\Omega) D_{M_1 K_1}^{I_1}(\Omega) D_{M_2 K_2}^{I_2}(\Omega) D_{M_3 K_3}^{I_3}(\Omega). \quad (29)$$

The integral can be calculated with the aid of the following Clebsch-Gordan series [7]:

$$D_{M_1 K_1}^{J_1}(\Omega) D_{M_2 K_2}^{J_2}(\Omega) = \sum_{J_3=|J_1-J_2|}^{J_1+J_2} \sum_{M_3 K_3} \mathbf{C}_{J_1 M_1 J_2 M_2}^{J_3 M_3} D_{M_3 K_3}^{J_3}(\Omega) \mathbf{C}_{J_1 K_1 J_2 K_2}^{J_3 K_3}. \quad (30)$$

This gives

$$V_{IMK}^{2B,2} = \sum_{I_1 M_1 K_1} \tilde{V}_{I_1 M_1 K_1}^{2B} \sum_{I_2 M_2 K_2} c_{I_2 M_2 K_2}^{\mathcal{N}} \sum_{I_3 M_3 K_3} c_{I_3 M_3 K_3}^{\mathcal{N}} \sum_{I''=|I_2-I_3|}^{I_2+I_3} \sum_{M'' K''} \mathbf{C}_{I_2 M_2 I_3 M_3}^{I'' M''} \mathbf{C}_{I_2 K_2 I_3 K_3}^{I'' K''} \frac{2I+1}{8\pi^2} \int d\Omega D_{MK}^{I*}(\Omega) D_{M_1 K_1}^{I_1}(\Omega) D_{M'' K''}^{I''}(\Omega). \quad (31)$$

Eventually, after using expression (23), we obtain

$$V_{IMK}^{2B,2} = \sum_{I_1 M_1 K_1} \left\{ \sum_{I_2 M_2 K_2} c_{I_2 M_2 K_2}^{\mathcal{N}} \sum_{I_3 M_3 K_3} c_{I_3 M_3 K_3}^{\mathcal{N}} \right. \\ \left. \sum_{I''=|I_2-I_3|}^{I_2+I_3} \sum_{M''K''} c_{I_2 M_2 I_3 M_3}^{I''M''} c_{I_2 K_2 I_3 K_3}^{I''K''} c_{I_1 M_1 I''M''}^{IM} \right. \\ \left. c_{I_1 K_1 I''K''}^{IK} \right\} \tilde{V}_{I_1 M_1 K_1}^{2B} \equiv \sum_{I_1 M_1 K_1} A_{I_1 M_1 K_1}^{IMK} \tilde{V}_{I_1 M_1 K_1}^{2B} \quad (32)$$

with the following selection rules on intermediate summations:

$$M_2 + M_3 = M'', \quad M_2 + M_3 = M'', \\ M_1 + M'' = M, \quad K_1 + K'' = K. \quad (33)$$

From the practical point of view, it is important to notice that the intermediate summations over  $I'', M'', K''$  can be extended as,

$$\sum_{I''=|I_2-I_3|}^{I_2+I_3} \longrightarrow \sum_{I''=0}^{2J}, \quad (34)$$

with the added terms being zero owing to properties of the Clebsch-Gordan coefficients. This allows us to change in Eq. (32) the order of summations, and to split the multi-dimensional summations into two independent sets of sums, that is,

$$A_{I_1 M_1 K_1}^{IMK} = \sum_{I''M''K''} X_{M''K''}^{I''} c_{I_1 M_1 I''M''}^{IM} c_{I_1 K_1 I''K''}^{IK}, \quad (35)$$

where

$$X_{M''K''}^{I''} = \sum_{I_2 M_2 K_2} c_{I_2 M_2 K_2}^{\mathcal{N}} \sum_{I_3 M_3 K_3} c_{I_3 M_3 K_3}^{\mathcal{N}} \\ c_{I_2 M_2 I_3 M_3}^{I''M''} c_{I_2 K_2 I_3 K_3}^{I''K''}. \quad (36)$$

The trick used above facilitates numerical calculations. It should also be noted that the Clebsch-Gordan coefficients impose selection rules that introduce further simplifications. For example, in Eq. (35), one has  $M'' = M - M_1$  and  $K'' = K - K_1$ , meaning that corresponding summations are effectively one-dimensional.

In the applications of our QR scheme, we used a strategy similar to the one used for the LR scheme, that is, energies  $E_{I=0}$  and sum-rule residuals were investigated as a functions of  $I_{\max}$ , which is the maximum value of angular momentum admitted in the summations in Eqs. (35) and (36).

First, we applied the QR method to the SIII case, already analyzed in Sec. IIB in the context of the LR method, see Fig. 3. In this case, both regularization schemes are fully equivalent and give identical results. This not only tests the code but also speaks in favor of the reliability of both schemes.

Next, we applied both regularization schemes to the case of the SLy4 functional [28], which features a

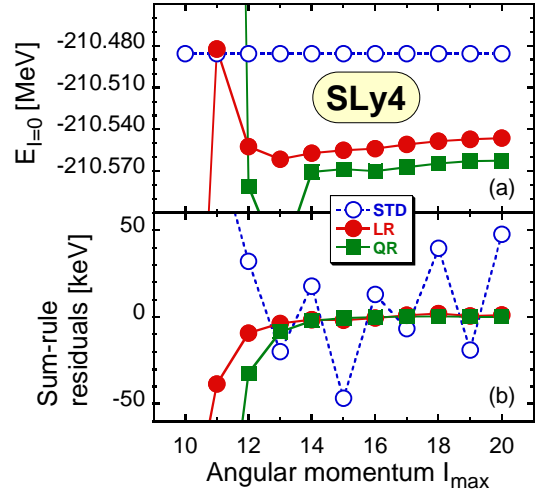


FIG. 5. (Color online) Same as in Fig. 1 but for the SLy4 Skyrme functional. Full squares represent results obtained using the QR method.

fractional-power density dependence with  $\eta = 1/6$ . The results are presented in Fig. 5. In this case, the regularization is insufficient to stabilize the energy of the lowest  $I=0$  state. By removing contributions coming from uncompensated poles in energy kernels, the QR scheme lowers the energy of the  $I = 0$  state as compared to the LR scheme. However, because of non-analyticity caused by the fractional power, it is unable to fully stabilize the solution.

### III. SUMMARY AND PERSPECTIVES

In this work, we proposed a method to regularize the two-body off-diagonal MR DFT kernels and we presented the first application thereof to a representative case of the angular-momentum projection. The method is based on two general assumptions:

1. First, it assumes that the MR EDF is regularizable, meaning in practice that there exist a regularization scheme replacing the kernel by its smooth counterpart that can be expanded in a set of Wigner  $D$ -functions (16). No explicit knowledge of the regularization scheme is required.
2. Second, it assumes that the singularities, which appear in the denominator of the two-body kernel, originate from vanishing overlap, which is a result of using the GWT. This allows us to identify terms proportional to  $\langle \Psi | \tilde{\Psi} \rangle^{-(1+\eta)}$ , where  $\eta$  comes from the direct density dependence of the generator of two-body kernel, as potentially the most dangerous ones.

The essential advantage of the method is in avoiding the necessity to explicitly remove the self-interactions [2, 3]. Instead, the proposed method relies on computing a set

of auxiliary integrals of non-singular kernels obtained by multiplying the original ones with an appropriately chosen power of the overlap. Provided that the GWT is the only source of singularities, the auxiliary integrals turn out to be linear functions of the true regularized matrix elements, and the entire problem can be reduced to an algebraic task of solving a set of linear equation. The method also has a certain internal flexibility, namely, it can be applied to selected parts of the EDF only. This feature is important in cases when troublesome parts of the EDF can be isolated. The example is the Coulomb exchange interaction treated within the Slater approximation.

A certain disadvantage of the method is the fact that, to achieve a desired accuracy, the auxiliary integrals require more quadrature nodes. In addition, one has to invert or perform the SVD decomposition of the auxiliary matrices  $A$ , see Eqs. (25) and (35)), which can be a potential source of numerical inaccuracies. Both problems become more acute with increasing power of the overlap multiplying the kernel. Nevertheless, in this exploratory study we have demonstrated that both the LR and QR schemes can be realized. Problems encountered for the calculations involving the SLy4 functional

reflect the inadequacy of the scheme in applications to fractional-power density-dependent terms, which lead to non-analytic dependence of kernels on the Euler angles.

Finally, an interesting feature of our calculations is that they reveal the fact of how much the effects of using EDFs that are not derived from *true* interactions can be inconspicuous. Our calculations show that even the slightest departure from the *true* interaction is immediately detectable through the sum rules, but it can be completely invisible when looking at energies of low-lying states, which are often perfectly stable.

## ACKNOWLEDGMENTS

This work was supported in part by the Polish National Science Centre (NCN) under Contract No. 2012/07/B/ST2/03907, by the THEXO JRA within the EU-FP7-IA project ENSAR (No. 262010), by the ERANET-NuPNET grant SARFEN of the Polish National Centre for Research and Development, and by the Academy of Finland and University of Jyväskylä within the FIDIPRO programme.

- 
- [1] J. Dobaczewski, M. V. Stoitsov, W. Nazarewicz, and P.-G. Reinhard, Phys. Rev. C **76**, 054315 (2007).
  - [2] D. Lacroix, T. Duguet, and M. Bender, Phys. Rev. C **79**, 044318 (2009).
  - [3] M. Bender, T. Duguet, and D. Lacroix, Phys. Rev. C **79**, 044319 (2009).
  - [4] J. Blaizot and G. Ripka, *Quantum theory of finite systems* (MIT Press, Cambridge Mass., 1986).
  - [5] M. Rafalski, *et al.*, unpublished.
  - [6] P. Ring and P. Schuck, *The Nuclear Many-Body Problem* (Springer, 1980).
  - [7] D. Varshalovich, A. Moskalev, and V. Khersonskii, *Quantum Theory of Angular Momentum* (World Scientific, Singapore, 1988).
  - [8] T. Skyrme, Phil. Mag. **1**, 1043 (1956).
  - [9] T. Skyrme, Nucl. Phys. **9**, 615 (1959).
  - [10] D. Gogny, Nucl. Phys. **A237**, 399 (1975).
  - [11] P. Bonche, J. Dobaczewski, H. Flocard, P.-H. Heenen, and J. Meyer, Nucl. Phys. **A510**, 466 (1990).
  - [12] L. M. Robledo, Int. J. Mod. Phys. E **16**, 337 (2007).
  - [13] L. M. Robledo, J. Phys. **G 37**, 064020 (2010).
  - [14] K. Schmid, Prog. Part. Nucl. Phys. **52**, 565 (2004).
  - [15] T. Duguet, Phys. Rev. C **67**, 054308 (2003).
  - [16] H. Zduniczuk, J. Dobaczewski, and W. Satuła, Int. J. Mod. Phys. E **16**, 377 (2007).
  - [17] N. L. Vaquero, J. L. Egido, and T. R. Rodríguez, Phys. Rev. C **88**, 064311 (2013).
  - [18] M. Beiner, H. Flocard, N. V. Giai, and P. Quentin, Nucl. Phys. A **238**, 29 (1975).
  - [19] W. Satuła, J. Dobaczewski, W. Nazarewicz, and M. Rafalski, Phys. Rev. Lett. **106**, 132502 (2011).
  - [20] K. Washiyama, K. Bennaceur, B. Avez, M. Bender, P.-H. Heenen, and V. Hellema, Phys. Rev. C **86**, 054309 (2012).
  - [21] J. Sadoudi, M. Bender, K. Bennaceur, D. Davesne, R. Jodon, and T. Duguet, Phys. Scr. **T154**, 014013 (2013).
  - [22] K. Bennaceur, J. Dobaczewski, and F. Raimondi, (2013), arXiv:1305.7210.
  - [23] B. Bally, “Description of odd-mass nuclei by multi-reference energy density functional methods,” (2014), Thèse présentée pour obtenir le grade de Docteur ès Sciences de l’Université de Bordeaux, unpublished.
  - [24] B. Bally, B. Avez, M. Bender, and P.-H. Heenen, (2014), arXiv:1406.5984.
  - [25] J. Slater, Phys. Rev. **81**, 385 (1951).
  - [26] J. Dobaczewski, W. Satuła, B. Carlsson, J. Engel, P. Olbratowski, P. Powłowski, M. Sadziak, J. Sarich, N. Schunck, A. Staszczak, M. Stoitsov, M. Zalewski, and H. Zduniczuk, Comput. Phys. Commun. **180**, 2361 (2009).
  - [27] N. Schunck, J. Dobaczewski, J. McDonnell, W. Satuła, J. Sheikh, A. Staszczak, M. Stoitsov, and P. Toivanen, Comput. Phys. Commun. **183**, 166 (2012).
  - [28] E. Chabanat, P. Bonche, P. Haensel, J. Meyer, and R. Schaeffer, Nucl. Phys. **A627**, 710 (1997).